The International Journal of Advanced Manufacturing Technology (2020) 107:4427–4436
https://doi.org/10.1007/s00170-020-05349-z

ORIGINAL ARTICLE

High deposition efficiency and delamination issues during high-pressure cold spraying metallization of PEEK using spherical copper powders

Libin Lalu Koithara[1] · Rija Nirina Raoelison[1] · Sophie Costil[1] · Xinliang Xie[1]

Received: 22 November 2019 / Accepted: 17 April 2020 / Published online: 28 April 2020

Abstract
Achieving high deposition efficiency (DE) is a current challenge of cold spraying metallization of polymers for developing surface function such as a conduction performance. Low-pressure cold spraying (LPCS) has been explored for that purpose but meets DE limitation less than 50% generally. This paper focuses on the possibility to overcome this issue, but using high-pressure cold spraying (HPCS). The anchoring of the copper powders onto the PEEK substrate is not difficult, but the deposition can fail during the coating build-up. A high pressure of 2.5 MPa without a gas preheating does not produce a coating build-up. Higher chamber pressures are required, but this implies to increase the gas temperature up to 400 °C to reach high deposition efficiency up to 70%. However, the absorption of the impact energy by the PEEK substrate during the collision of the powders generates an intermediate weakly bonded layer which is characterized by a decohesion between weakly deformed powders. This structure impairs the integrity of the coating during the additive deposition. Spalling damage occurs. Therefore, the deposition becomes very sensitive to delamination issues to overcome.

Keywords Cold spraying · PEEK metallization · Deposition efficiency · Copper · Delamination

1 Introduction

PEEK polymer has gained more popularity among many organic thermoplastic polymers owing to its excellent ability to withstand wear and friction with remarkable thermal stability [1–3]. This material is also increasingly used as a bearing and sliding component to meet the best possible combination of lightweight and high-strength requirements [4, 5]. Currently, it is being used for various applications such as bearings, piston parts [2] or medical orthopaedic implants [6, 7] using the benefits of surface metallic functionalization. Today, there are various techniques of polymers metallization. Physical vapour deposition, chemical vapour deposition or electrodeposition are suitable for a thin metallization but can be costly [8–12]. The thermal spraying represents an alternative method that uses a kinematic deposition of micron-sized powders with the advantage of being a fast metallization process with a low release of materials. The kinetic energy of the powders can be generated by means of combustion flame jet (flame spraying), thermal jet combined with an electric discharge (electric arc spray) or ionized gas jet (plasma spraying). These methods have been experienced for metalizing polymers but the temperature processing (2000–14000 °C) involves a severe risk of exposure to high temperature that implies a careful deposition because of the thermal sensitivity of polymers [12]. Among the thermal spraying methods, the principle of supersonic expansion of a gas flow across a divergent nozzle allows a low temperature deposition with a high acceleration of the micron-sized powders. This capability has led to a wide development of polymer metallization by cold spraying.

The cold spray additive manufacturing has been successfully tested on various polymers including PEEK and enables metallic powders to form a coating [12–19]. Copper metallization was performed on diverse polymers to confer an electrical conductivity [13, 20–22], tribological properties [20], an intermediate bonding function [14, 15, 23], an antifouling reaction [24], antibacterial properties [25, 26] and further

✉ Rija Nirina Raoelison
rija-nirina.raoelison@utbm.fr

[1] Laboratoire Interdisciplinaire Carnot de Bourgogne, UMR 6303 CNRS, Université de Bourgogne Franche-Comté – UTBM, 90100 Belfort, France

functional performances the copper structure can generate [4]. There are several successful metallization feasibilities that mostly use a safe deposition to avoid a degradation of the polymer substrate during the cold spray metallization. A deposition with a low impact energy and low temperature can prevent a strong erosion or damage of the polymer. The suitability of a few μJ impact energy to ensure a successful deposition [23] explains the wide development of low-pressure cold spraying (LPCS) as metallization solution in the literature [13, 14, 16, 17, 23, 27–29]. The next milestone is to overcome an issue of weak deposition efficiency (DE) involved by a dissymmetry of mechanical properties between the metal powders and the polymer substrate.

Generally, the LPCS deposition suffers from a weak DE due to kinematic deficiency. There is a competition between bonding and erosion phenomena [17, 23, 28, 29], and increasing the gas pressure can alter the coating formation because powders do not reach the critical velocity of adhesion [28, 29]. The DE decreases during the continuous multiple impacts and makes tricky the control of the deposition. The typical DE range is about 10–30%. The challenges of LPCS are then to identify suitable conditions capable for minimizing or deleting this erosion phenomenon. A basic solution is to reduce the critical velocity level by using fine powders or soft metals. The choice of fine powders is generally supported by a theoretical argument that shows perspectives of high in-flight particle velocity. Powder size less than 5 μm is theoretically appropriate, but in practice, such powders meet various difficulties including a bad flowability, an easy clogging, a trajectory deviation due to a sensitivity to turbulences of the flow, and a sparse velocity distribution [17, 30–32]. Therefore, higher powder sizes are considered in the literature of LPCS that uses a typical granulometry of about d50 = 20 μm. With this restriction, the selection of potential solutions relies on the other features of the powder, and basically, on the material nature or on the powder morphology. Spherical copper powders with a size of d50 = 20 μm give a very low DE of about 10% even lower when using a pressure of 0.6 MPa [33]. A LPCS deposition of spherical aluminium powders (d50 = 17 μm) gives the same tendency with a DE of 7% [27]. Perspectives of DE improvement becomes possible when using a mixture with a softer material such as zinc and tin [17, 29, 34]. DE of 40% can be obtained with a high proportion of such soft metals but with this unbalanced ratio, the property of the coating is strongly deviated from the property of the functional material of the powder mixture [28].

Some studies combined the selection of powder features with the use of an undercoat layer to bond the functional coating to the polymer substrate. This solution is found to ease the coating build-up. Deposition of copper dendritic powders onto an intermediate layer made of copper or tin spherical powders facilitates the metallization of polymers [13, 14]. The dendritic morphology provides a double positive effect as reported in a literature review [35]. The irregular shape causes an efficient boundary layer separation across the powder media and generates thereby higher drag coefficient for a maximized velocity. During the collision, the dendritic shape increases the adhesion capability of the powders thanks to a better plastic deformation [36]. The rebound and erosion phenomena are then reduced. These advantages encouraged the use of dendritic powder for the LPCS metallization of polymers [21, 36–38] but do not enable to increase the DE beyond 40% [38]. Combination of various sublayers made of different powders granulometry represents also a solution for optimising the DE during LPCS. The optimisation of both gradient of sublayers and gas parameters increases the deposition efficiency, but the highest reachable value remains below 40% in spite of careful choice of the powder size for each sublayer [16]. The major conclusion of polymer metallization using LPCS is that despite various exploratory improvements for promoting the coating built-up, the deposition efficiency is limited to about 50%. In addition, the coating formation can also suffer from a delamination during the LPCS deposition [16]. Together, these limitations of the LPCS deposition have motivated the exploration of high-pressure cold spraying (HPCS).

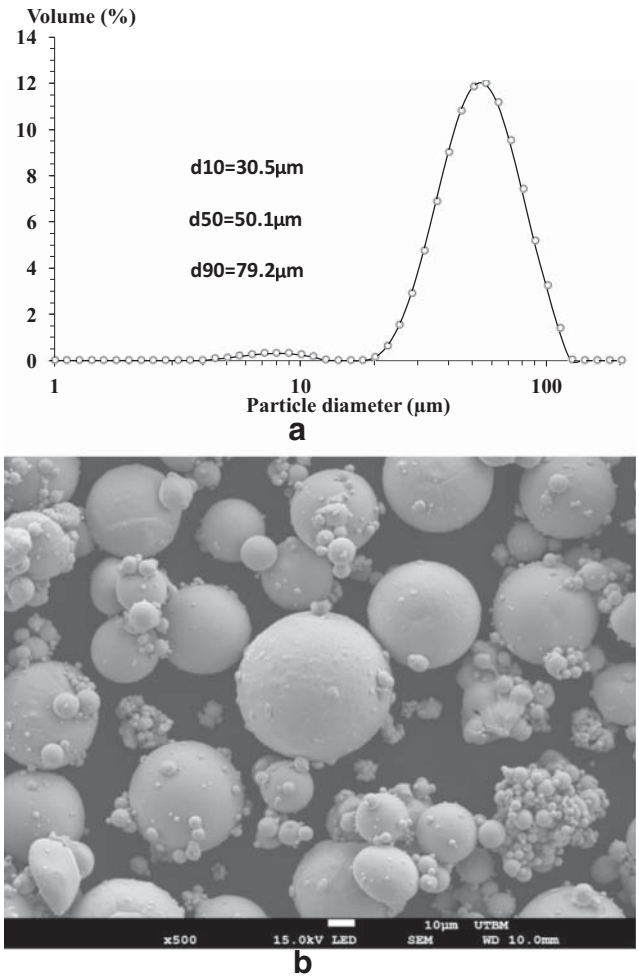

Fig. 1 Granulometry of the powders (**a**) and SEM observation (**b**)

Table 1 Process parameters for the CS deposition

Gas conditions	Pgas (MPa)	Tgas (°C)	SoD (mm)	Vnozzle (mm/s)	IncD (mm)	No. of cases
Unheated	2.5	29	45	500	3	(C1)
Preheated	3.0	200	75			(C2)
		400	105			(C3)

In the literature of HPCS metallization of polymers, a few studies alone are available. They have been recently published and are mostly focused on copper or aluminium deposition [22, 39] using the standard powder granulometry of CS and a gas setting up to (2.4 MPa, 3050 °C) for copper powders and (4 MPa, 350 °C) for aluminium powders. The first powders adhere onto the polymer surface by mechanical anchoring and enable the next powders to form a coating which can be thick up to a few millimetres. However, the exposure to high pressure and high temperature may involve structural distortion, erosion, or coating degradation by delamination. These are undesirable effects that prevent the obtention of a good coating [22, 39] and imply a tricky elaboration of deposition condition for a coating build-up free of degradation [39]. In addition, the suitable HPCS parameters suitable for a high DE are also a current issue. This paper explores the capability of HPCS to reach high DE through a variation of the gas setting on a HPCS system, from low pressure and low temperature towards high pressure and high temperature with an appropriate change of the standoff distance. The coating build-up or degradation phenomenon is also discussed to specify the difficulty of HPCS metallization of a polymer substrate. We focus our analysis on the copper deposition onto PEEK that is a typical hybrid case of interest in the field of cold spray metallization.

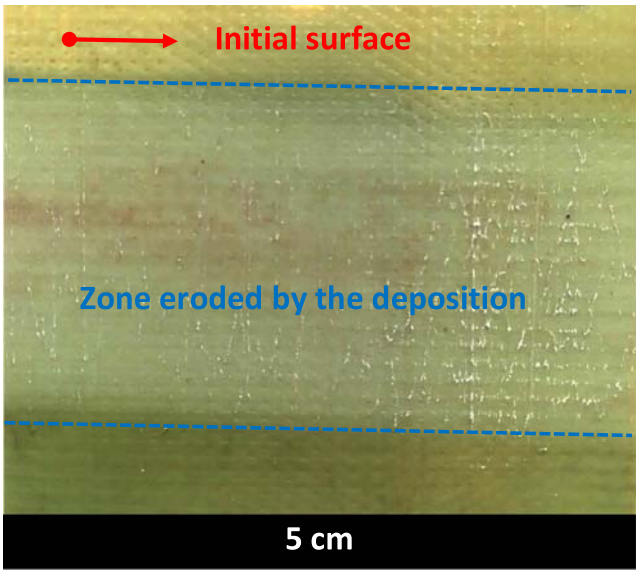

a

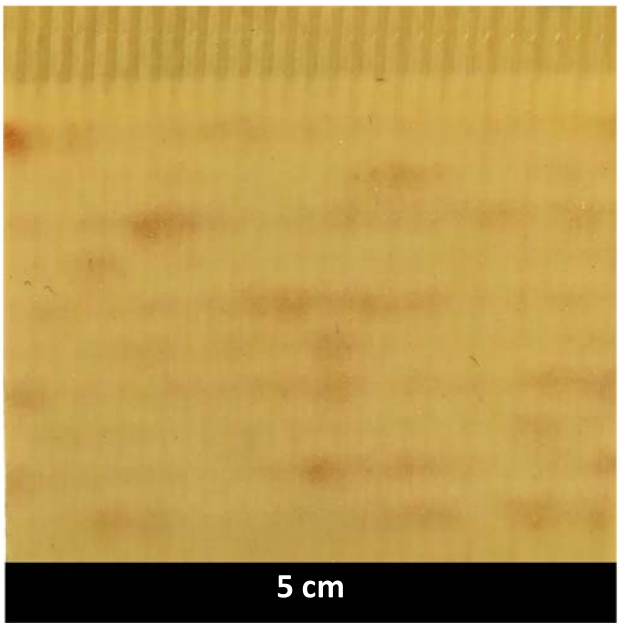

b

Fig. 2 Deposition with unheated gas (case C1). **a** Erosion of the PEEK surface after 2 passes. **b** Few traces of bonded copper after 5 passes

2 Materials and methods

Beige opaque PEEK (Polyether ether ketone) sheets acquired from RS-PRO are used as substrate. The samples have a dimension of 50 mm × 50 mm × 5 mm and are cleaned with ethanol before the deposition without any other surface preparations.

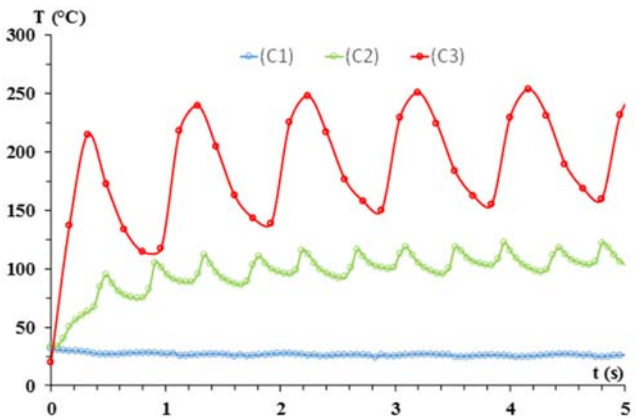

Fig. 3 Substrate temperature level of the PEEK surface for the different deposition conditions C1–C3, measured by the FLIR thermal camera at the centre of the substrate surface during the repetitive tracks

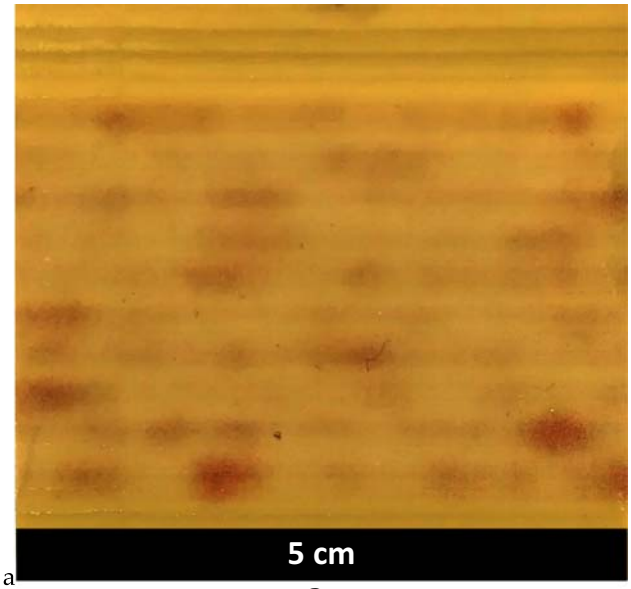

a

a

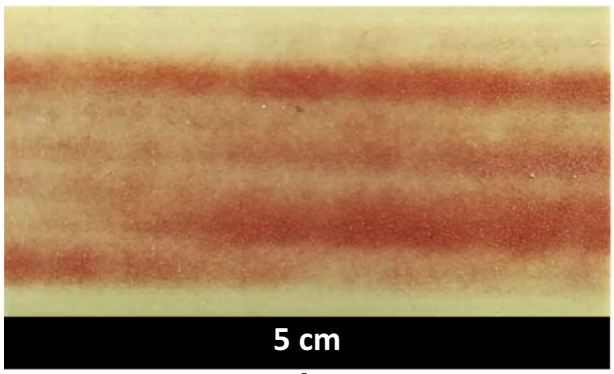

b

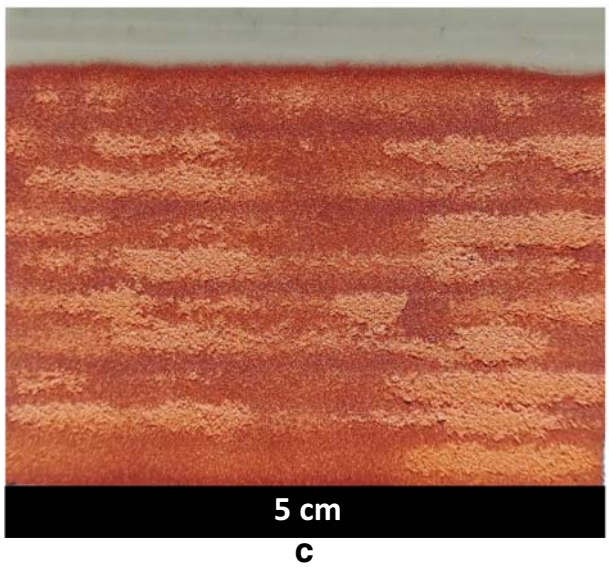

c

Fig. 4 Deposition with heated gas (case C2). **a** Few traces of bonded copper after 1 pass, **b** onset of bonding layer after 2 passes and, **c** irregular formation of the coating after 5 passes due to selective erosion

PEEK used is a semi-crystalline thermoplastic exhibiting melting point of 323 °C and glass transition temperature of 166 °C we characterized from a DCS analysis. The powder feedstock consists of spherical copper powders generated in-house (LERMPS) by gas atomization. The granulometry is specified on Fig. 1. The HPCS experiments are performed using a cold spray Kinetic 3000 system with air as propellant gas. The working pressure ranges from 1 to 3 MPa. The powders are axially fed into a MOC

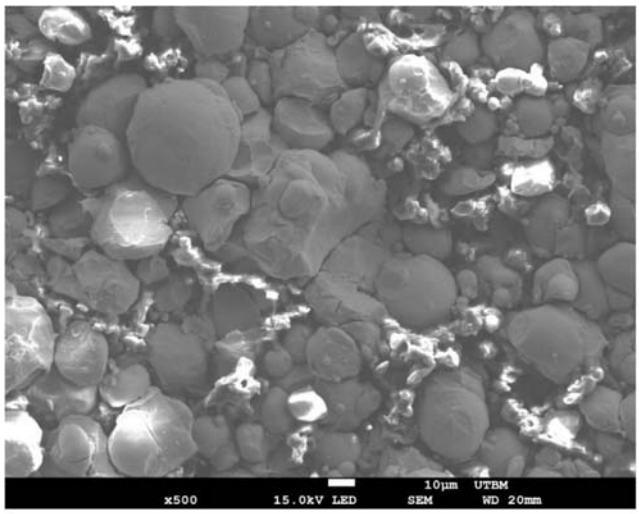

(a)

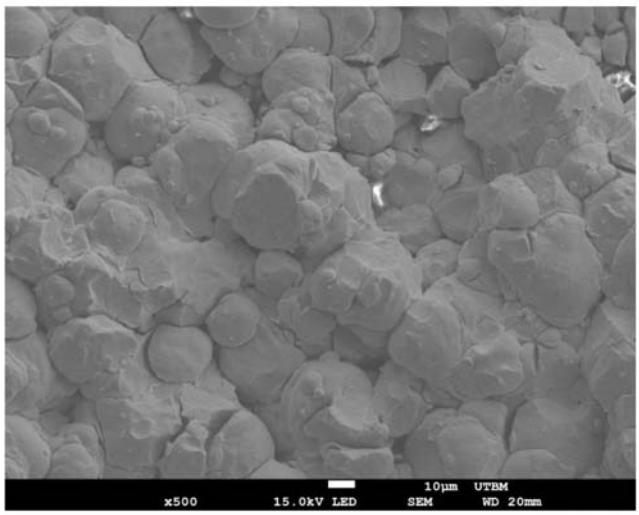

(b)

Fig. 5 Deposition with heated gas (case C2). **a** Bonding layer at the interface showing PEEK traces (bright zone) due to the indentation of powders, powders anchored onto the substrate, powders that remain spherical (apparent larger size) but anchored onto the substrate, fine powders that were deformed during the collision but without intercohesion, trace of craters due to collision of big powders, and finer craters due to erosion. **b** Top view of the incrementally coated layer showing weak deformation of powders with decohesion at their interfaces and trace of craters

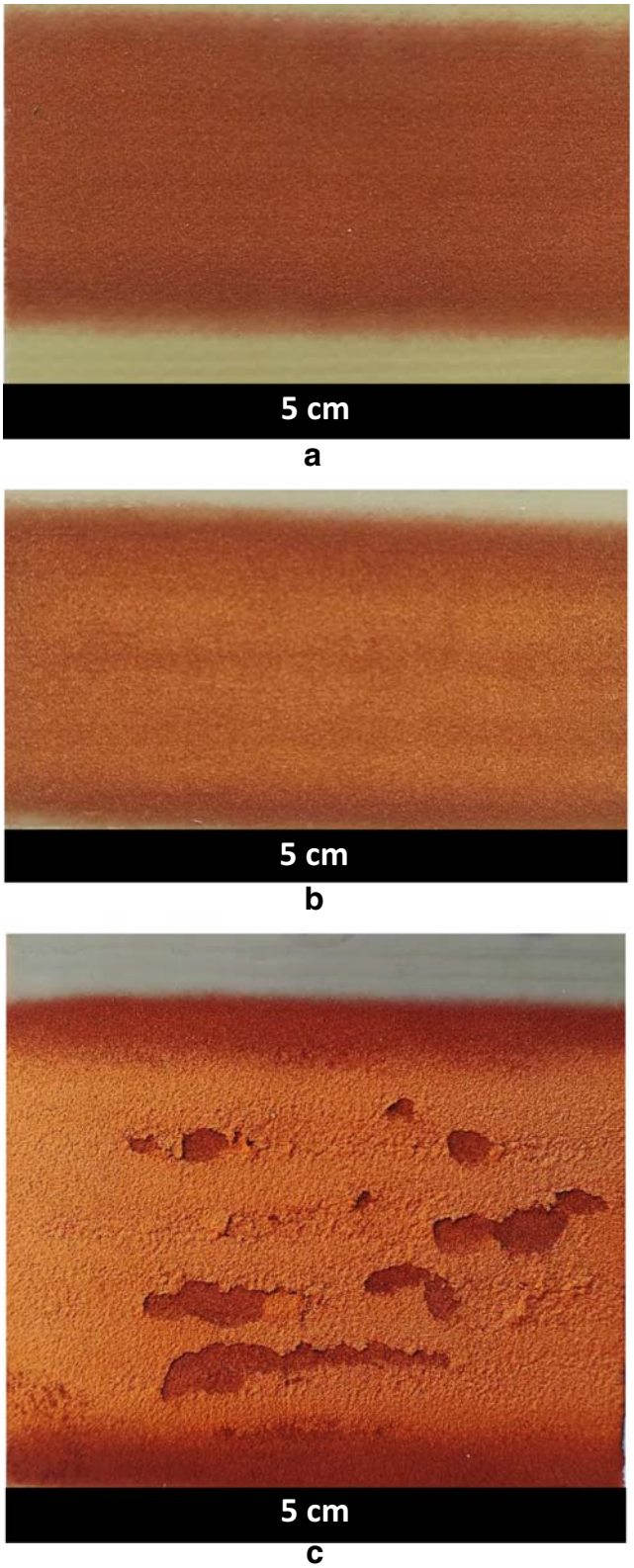

Fig. 6 Deposition with heated gas (case C3). **a** Formation of a bonded layer after one pass with a DE of 60%. **b** Reduction of the DE to 52% during a two-passes deposition due to competition between bonding and erosion. **c** Formation of the coating after 5 passes with the occurrence of delamination by spalling (DE = 70%)

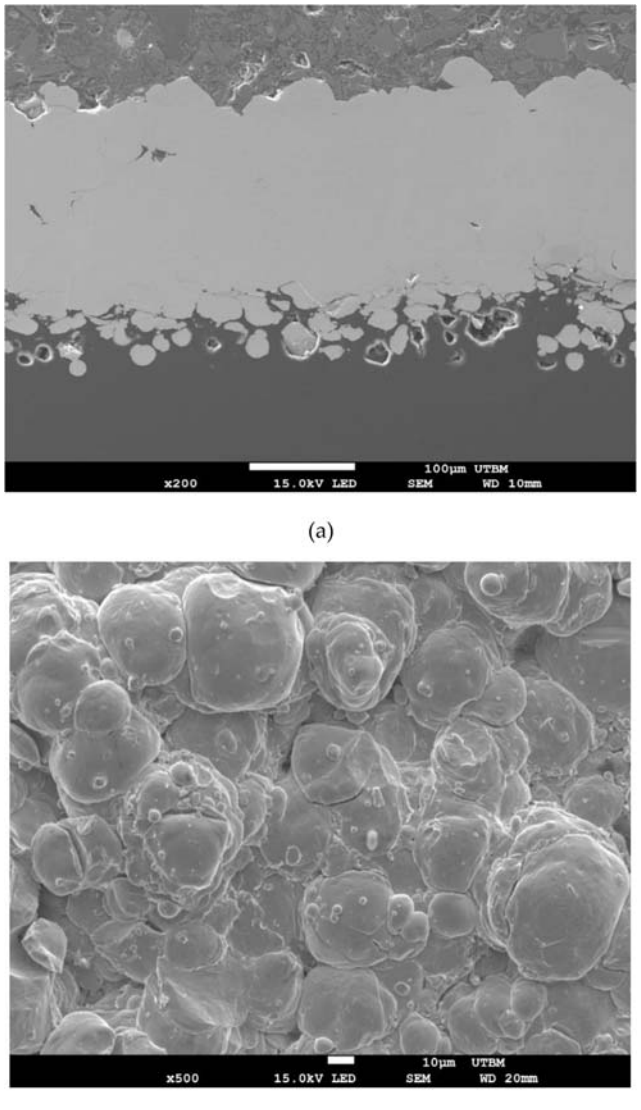

Fig. 7 Copper coating about 160 µm thick with a DE of 70% using the C3 deposition (**a**) and top view of the coating showing flattened powders and thereby plastic deformation that improves the coating build-up (**b**)

24 De Laval nozzle which has the following dimensions: an inlet diameter of 18 mm, a throat diameter of 2.7 mm, an outlet diameter of 7.8 mm, a convergent part length of 42 mm and a divergent part length of 130 mm. The deposition conditions consist of comparative cases that enable for finding a high DE achievable with this CS system. A classical way of DE measurement has been adopted. The DE value is the mass ratio between deposited powders and initial powder feedstock, using the initial weight of the substrate and the weight of the substrate + coating after emptying the powder feedstock. The experiment starts with an unheated gas that is generally suitable for temperature-sensitive materials such as polymers to prevent undesirable thermal effects. The highest gas pressure achievable on the CS system is 2.5 MPa without a gas preheating. This deposition is performed

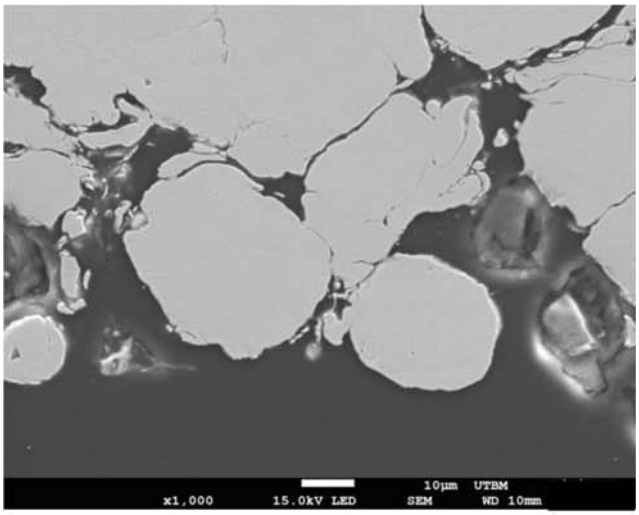

(a)

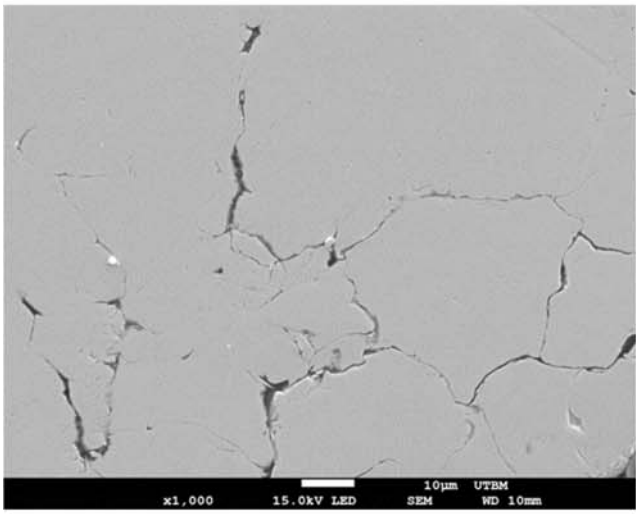

(b)

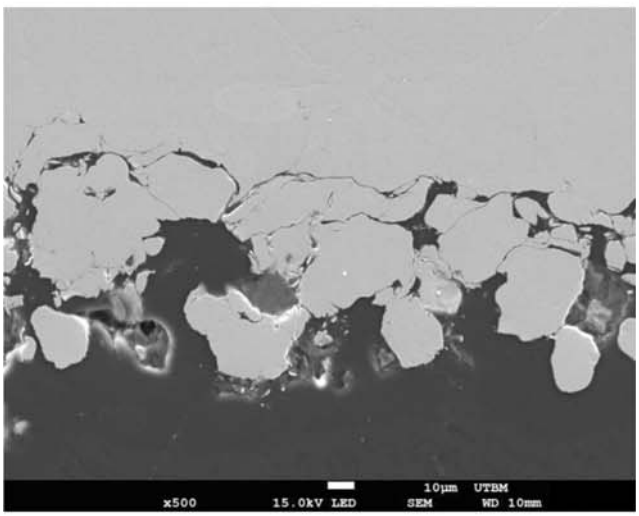

(c)

◀ **Fig. 8** Structure of the coating with the condition (case C3). **a** Anchoring onto the PEEK substrate without significant powders deformation. **b** Formation of the bonded layer with interfacial decohesion between deformed powders. **c** Coating build-up with better structural cohesion

with a standoff distance of 45 mm and a nozzle scanning velocity of 500 mm/s. The incremental displacement (denoted here IncD) of the nozzle between two successive tracks is 3 mm. A deposition cycle (denoted as pass) includes 10 tracks that are repeated 5 times to form a 5 passes coating. In addition, depositions with a single pass and two passes are also performed to investigate the process of coating build-up. For reaching high DE, we also explore the highest working pressure of 3 MPa along with increase in gas temperature that implies to use large standoff distances to protect the PEEK substrate from high thermal exposure. A blank test (without powders) gives the wall temperature of the substrate due to the parietal convective exchange with the impinging gas flow. The measurement is performed using the FLIR ONE thermal imaging system and an emissivity of 0.95 [40]. These different working conditions are summarized in Table 1.

3 Results and discussion

3.1 Coating formation and growth

Basically, the coating build-up during cold spraying occurs in two major steps: the formation of a 1st layer that is the adhesion of the powders on the substrate and then, the deposit growth governed by the cohesion between the powders during their additive collisions on the layer that was formed. Various mechanisms of deposit formation have been identified for diverse materials and different hybridizations in cold spray technology [4]. In case of soft substrate, the powders penetrate onto the substrate to produce a mechanical anchoring as bonding mechanism. Then, the metallic coating grows by metallic bonding on the 1st layer. During the copper metallization of PEEK as investigated in this paper, the deposition using unheated gas fails to form the 1st layer (Fig. 2a). The deposition leaves a few traces of rebound over the substrate surface as evidenced by the apparent colour change over the deposition surface. Competition between anchoring and erosion then makes difficult the formation of the coating albeit the pass number is increased (Fig. 2b). A few traces of coppers were observed on the substrate surface. Although the gas pressure level (2.5 MPa) is higher than the pressure level of LPCS, the copper powders do not reach enough velocity to be anchored on the PEEK surface whose temperature is about 29 °C according to the measurement using the FLIR thermal camera device (Fig. 3).

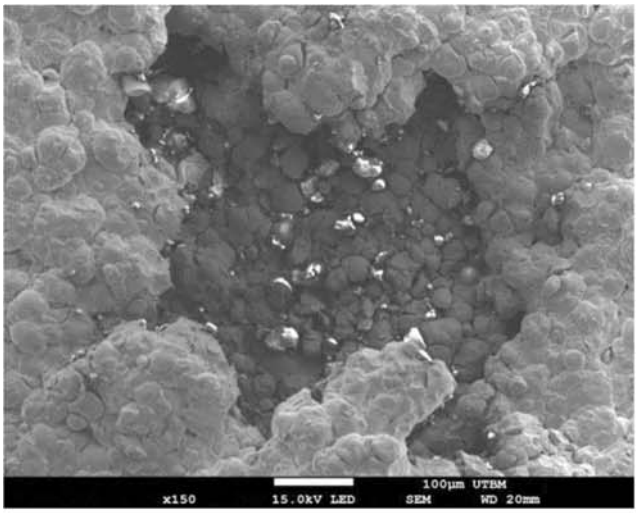

(a)

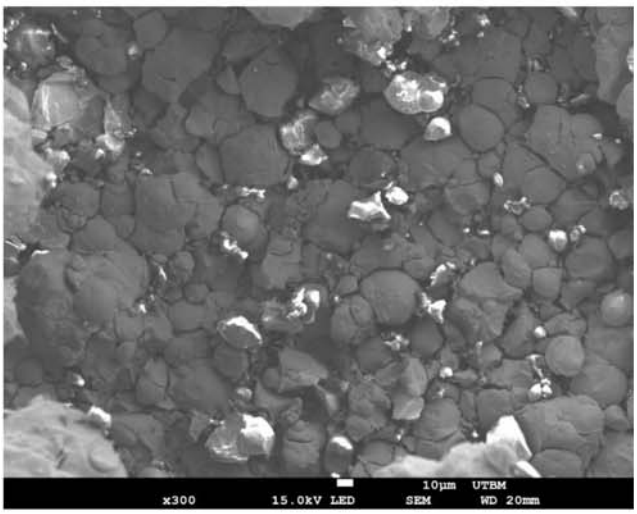

(b)

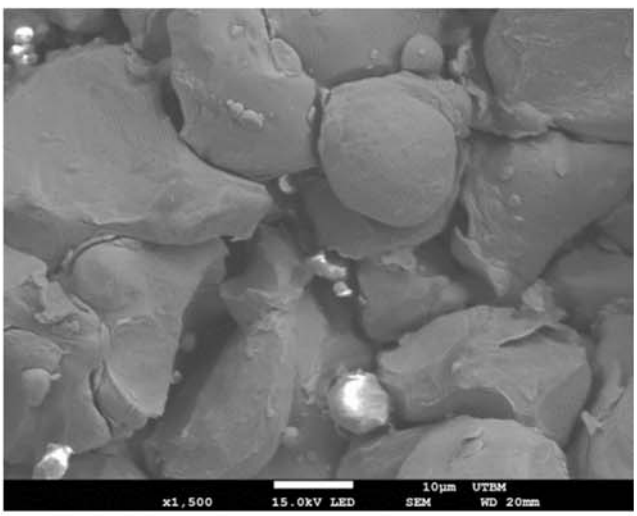

(c)

◀ **Fig. 9** Typical structure of a crater that characterizes a delamination by spalling (**a**), fragmentation of the bonded layer that forms a weakness zone under the coating (**b**) by interfacial decohesion between the powders (**c**)

When heating the propellant gas up to 200 °C, the substrate temperature reaches up to 130 °C (Fig. 3) and the inlet gas pressure slightly increases to 3 MPa providing better kinetic energy to the powders. The temperature oscillates due to the movement of the nozzle when passing across the measuring spot (Fig. 3). Although the substrate undergoes higher temperature, the one-pass deposition does not enable the formation of a 1st layer over the whole surface, due to the rebound and erosion phenomena. The copper powders adhere on some dispersed zone alone, without covering the whole surface subjected to the powders jet (Fig. 4a). Repeating the passes over and over progressively produces bonded layers by granulometry effect. Whereas large powders cause erosion, small-sized powders may achieve the required critical velocity of bonding. This event is governed by the random variation of powder size due the granulometry of the powder feedstock. Weakly bonded layer or random weakness zone is therefore generated by this granulometry effect. Some powders are anchored into the substrate and form discontinuous bonded layer during the second pass (Fig. 4b). This promotes a heterogeneous coating build-up (Fig. 4c). Then, during the additive deposition, a part of the powders adheres on the former bonded copper layer while the other part rather causes random erosion because of kinematic deficiency. In Fig.4c, the eroded zone is revealed by the darker copper area while the brighter one corresponds to the incrementally coated layer. Note that the erosion persists with the repetition of the deposition due to the variance of powder velocity by granulometry effect. In addition, the absorption of the collision by the PEEK can also impair the copper/copper bonding. Since the PEEK substrate is prone to deformation, the copper powders are less deformed during the development of the first layers. Due to insufficient plastic deformation, powders are not bonded to each other during the multiple collisions and erode the formerly coated layer. The competition between deformation, bonding, and erosion are evidenced in (Fig. 5a). A SEM top view of the coating shows a structure of a bonded layer composed of some features: PEEK traces (bright zone) that emerge due to the indentation of powders, powders that were anchored in the substrate, powders that remain spherical (apparent larger size) but anchored in the substrate, powders (apparent finer size) that were deformed during the collision but without inter-cohesion, traces of craters due to collision of big powders, and finer craters due to erosion. On an incrementally coated layer (brighter zone of Fig. 4c), deformed powders were observed with bonded and unbonded interfaces (Fig. 5b). Craters also appear due to the erosion of the unbonded powders.

To improve the coating build-up, the gas is preheated up to 400 °C because the pre-chamber pressure cannot be further increased. The gas stream heats the substrate up to about 240 °C (Fig. 3) that is conducive to a thermomechanical softening since this temperature level exceeds the glass transition temperature of the PEEK substrate despite that it is under the PEEK melting point. Combined with the increased velocities of the powders, this thermal effect enhances the mechanical anchoring onto the PEEK to form a bonded layer that immediately covers the deposition surface in a single pass (Fig. 6a), with a DE of 60%. The copper/copper collision that starts from this bonded layer enables a continuous and regular coating build-up as long as the structural cohesion within the deposit resists to erosion. During a two-passes deposition, the coating formation is continuing (Fig. 6b) but the DE slightly decreases down to 52% due to an erosion. After the five-passes deposition, the coating reaches a thickness of 160 μm (Fig. 7b) with a high DE of 70%. The gas condition (400 °C, 3 MPa) promotes better plastic deformation as observed on the top view of the deposit (Fig. 7c). The powders are more flattened that was not reached using the gas setting of 200 °C and 3 MPa (Fig. 5b). However, some bad inter-cohesion remains between the powders although they get more deformed. Furthermore, the coating formation at (400 °C, 3 MPa) suffers from another erosion type. Delamination appears and the failure zones exhibit large spalls (Fig. 6c).

3.2 Mechanism of delamination by spalling

Due to lower mechanical property compared to the copper, the PEEK substrate absorbs the collision that creates bad bonding between copper powders during the formation of the 1st layer (Fig. 8). Therefore, a gradient of weak deformation of copper powders across the PEEK/copper interface causes a delamination during the repetitive passes. As discussed in the previous section, the penetration of the copper into the PEEK substrate generates an intermediate layer characterized by unbonded powders due to insufficient plastic deformation. A cross-section observation shows this typical evolution of powder behaviours, that is, a nearly unchanged shape (spherical) due to the anchoring onto the soft PEEK (Fig. 8a), and then a deformed shape but with bad bonding during the copper/copper collision (Fig. 8b). Despite this weak bonding, the deposit grows until this intermediate weakly bonded layer gets thick enough to produce a mechanical barrier against the absorption of the collision by the PEEK substrate. Thus, the dissymmetry of mechanical behaviour decreases and then the copper/copper collision enables the mutual plastic deformation that promotes inter-cohesion within the coating (Fig. 8c). This gradient of structure impairs the integrity of the coating during the additive deposition that becomes very sensitive to delamination. Spalling damage occurs because of overload stress produced by the multiple collisions. In addition, the PEEK substrate acts as a thermal barrier due to its low thermal conductivity so that the confinement of heat within the coating is conducive to a thermomechanical softening that can facilitate a spalling during the deposition. The incrementally created layer becomes sensitive to the collision stresses and breaks at the weakness zones.

The spalling produces craters, random in terms of location and size (Fig. 6c). Basically, the normal pressure of the impinging flow does not significantly change during the nozzle transverse motion since the gas pre-chamber pressure and temperature remains constant during the deposition. The random formation of the weakness zone within the coating is therefore attributed to the random distribution of the intermediate weakly bonded layer due to the granulometry effect. The

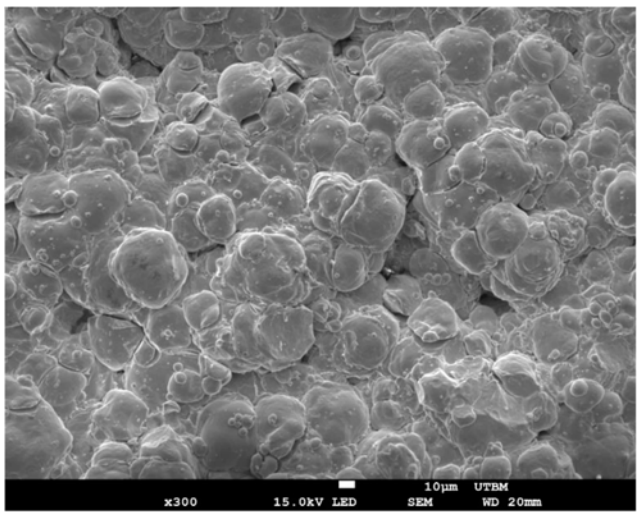

(a)

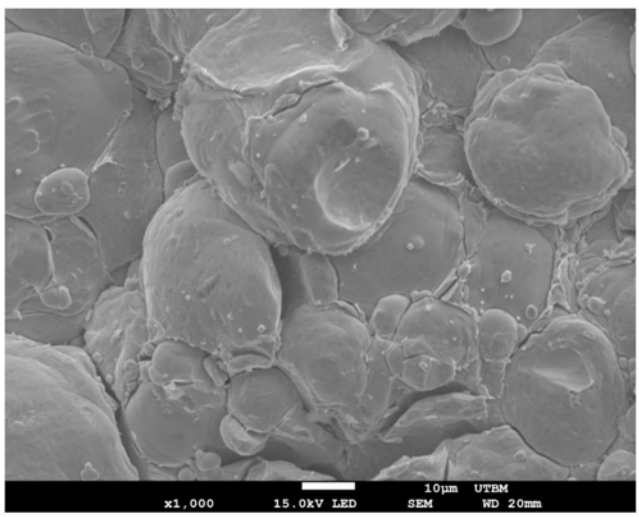

(b)

Fig. 10 Top view of the deposit showing inter-powder decohesion during the coating build-up despite of powders flattening: formation of weak bonding that breaks during the spalling (**a**) and magnified view of both inter-powders weak bonding and decohesion (**b**)

powder size ranges in between 4 and 126 μm as shown in Fig. 1b. The kinematic variance of these powders due this distribution generates the random formation of the weakness zone, and then the irregular spalling with large or little craters (Fig. 6c). However, the structure of the craters is similar and exhibits the same damage mechanism. Figure 9 shows SEM pictures of a typical crater with magnified views of the fracture. When subjected to the collision stresses, the defective bonding between powders causes the rupture of the coating. The spalling damage is characterized by a fragmentation within the intermediate weakly bonded layer (Fig. 9b) due to a powder/powder decohesion (Fig. 9c) that easily breaks the coating over the fragmented zone. The size of the spalling damage zone depends on crack formation and propagation in the transversal plan. This is also a random phenomenon governed by the presence of weakness zone due to the granulometry effect. SEM top views of the coating evidence unbonded region (Fig. 10a) and also powder/powder debonding (Fig. 10b) despite the occurrence of plastic deformation revealed by the observation of flattened powders. These defects activate the spalling and make difficult the cold spray manufacturing of good and thick copper coating on the PEEK substrate.

4 Conclusions

This study investigated the capability of cold spraying to reach high DE during a copper metallization of PEEK. Since PEEK material is thermally sensitive, some studies in the literature suggest using low-pressure cold spraying that ensures a low temperature deposition. The metallization is successful but suffers from a low DE, of about 40%, despite various improvements. In this paper, we suggested exploring the high-pressure cold spray metallization with three deposition conditions: (C1) high pressure and unheated gas (2.5 MPa–29 °C), (C2) high pressure and intermediate gas temperature (3 MPa, 200 °C), and (C3) high pressure with highly heated gas (3 MPa, 400 °C). The condition C1 fails to produce a coating. The copper powders adhere to some dispersed zone alone without covering the whole substrate surface subjected to the powders jet. With the deposition (C2), there is a coating build-up, but regular fine delamination occurs due to erosion. The competition between bonding and erosion can be explained by a variance of powder velocity due to the granulometry range and an absorption of the collision by the PEEK which is the softer part of the Cu/PEEK combination. The gas condition (C3) enables for generating continuous deposit formation with a DE up to 70%. Some elements to the understanding of the delamination that limits the DE are suggested. Even high DE in the range of 70% can be achieved; the coating formation clearly suffers from a delamination by spalling damage. This spalls formation is explained by the presence of an intermediate weakly bonded layer, the collision stresses on the substrate, and the confinement of the heat within the copper coating since the PEEK substrate acts as a thermal barrier due to its low thermal conductivity. The intermediate weakly bonded layer eases the delamination because of the decohesion of powders within this zone.

References

1. Chen X, Su Y, Reay D, Riffat S (2016) Recent research developments in polymer heat exchangers – a review. Renew Sust Energ Rev 60:1367–1386. https://doi.org/10.1016/j.rser.2016.03.024
2. Zhang G, Yu H, Zhang C, Liao H, Coddet C (2008) Temperature dependence of the tribological mechanisms of amorphous PEEK (polyetheretherketone) under dry sliding conditions. Acta Mater 56: 2182–2190. https://doi.org/10.1016/j.actamat.2008.01.018
3. Kurokawa M, Uchiyama Y, Nagai S (2000) Performance of plastic gear made of carbon fiber reinforced poly-ether-ether-ketone: part 2. Tribol Int 33:715–721. https://doi.org/10.1016/S0301-679X(00)00111-0
4. Raoelison RN, Verdy C, Liao H (2017) Cold gas dynamic spray additive manufacturing today: deposit possibilities, technological solutions and viable applications. Mater Des 133:266–287. https://doi.org/10.1016/j.matdes.2017.07.067
5. Raoelison RN (2018) Coeval cold spray additive manufacturing variances and innovative contributions. Cold-Spray Coat. Springer, Cham, pp 57–94. https://doi.org/10.1007/978-3-319-67183-3_3
6. Lee JH, Jang HL, Lee KM, Baek H-R, Jin K, Hong KS, Noh JH, Lee HK (2013) In vitro and in vivo evaluation of the bioactivity of hydroxyapatite-coated polyetheretherketone biocomposites created by cold spray technology. Acta Biomater 9:6177–6187. https://doi.org/10.1016/j.actbio.2012.11.030
7. Antibacterial property of cold-sprayed HA-Ag/PEEK coating | SpringerLink n.d. https://link.springer.com/article/10.1007/s11666-008-9283-0. Accessed 2 Oct 2019
8. Gritsenko KP (1993) Metal-polymer optical storage media produced by PECVD. Thin Solid Films 227:1–2. https://doi.org/10.1016/0040-6090(93)90177-Q
9. Duguet T, Senocq F, Laffont L, Vahlas C (2013) Metallization of polymer composites by metalorganic chemical vapor deposition of Cu: surface functionalization driven films characteristics. Surf Coat Technol 230:254–259. https://doi.org/10.1016/j.surfcoat.2013.06.065
10. Siegel J, Kotal V(2007) Preparation of thin metal layers on polymers. 10.14311/904
11. de Leeuw DM, Kraakman PA, Bongaerts PFG, Mutsaers CMJ, Klaassen DBM (1994) Electroplating of conductive polymers for the metallization of insulators. Synth Met 66:263–273. https://doi.org/10.1016/0379-6779(94)90076-0
12. Gonzalez R, Ashrafizadeh H, Lopera A, Mertiny P, McDonald A (2016) A review of thermal spray metallization of polymer-based structures. J Therm Spray Technol 25:897–919. https://doi.org/10.1007/s11666-016-0415-7
13. Ganesan A, Affi J, Yamada M, Fukumoto M (2012) Bonding behavior studies of cold sprayed copper coating on the PVC polymer substrate. Surf Coat Technol 207:262–269. https://doi.org/10.1016/j.surfcoat.2012.06.086
14. Ganesan A, Yamada M, Fukumoto M (2013) Cold spray coating deposition mechanism on the thermoplastic and thermosetting

polymer substrates. J Therm Spray Technol 22:1275–1282. https://doi.org/10.1007/s11666-013-9984-x
15. Robitaille F, Yandouzi M, Hind S, Jodoin B (2009) Metallic coating of aerospace carbon/epoxy composites by the pulsed gas dynamic spraying process. Surf Coat Technol 203:2954–2960. https://doi.org/10.1016/j.surfcoat.2009.03.011
16. Gillet V, Aubignat E, Costil S, Courant B, Langlade C, Casari P, Knapp W, Planche MP (2019) Development of low pressure cold sprayed copper coatings on carbon fiber reinforced polymer (CFRP). Surf Coat Technol 364:306–316. https://doi.org/10.1016/j.surfcoat.2019.01.011
17. Che H, Vo P, Yue S (n.d.) Metallization of carbon fibre reinforced polymers by cold spray. Surf Coat Technol 313:236–247. https://doi.org/10.1016/j.surfcoat.2017.01.083
18. Archambault G, Jodoin B, Gaydos S, Yandouzi M (2016) Metallization of carbon fiber reinforced polymer composite by cold spray and lay-up molding processes. Surf Coat Technol 300:78–86. https://doi.org/10.1016/j.surfcoat.2016.05.008
19. Njuhovic E, Witt A, Kempf M, Glöde S, Altstädt V (n.d.) Metallization of fiber-reinforced epoxy composites - effect of surface structure on the peel strength. 7
20. King PC, Poole AJ, Horne S, de Nys R, Gulizia S, Jahedi MZ (2013) Embedment of copper particles into polymers by cold spray. Surf Coat Technol 216:60–67. https://doi.org/10.1016/j.surfcoat.2012.11.023
21. Małachowska A, Winnicki M, Konat Ł, Piwowarczyk T, Pawłowski L, Ambroziak A, Stachowicz M (n.d.) Possibility of spraying of copper coatings on polyamide 6 with low pressure cold spray method. Surf Coat Technol 318:82–89. https://doi.org/10.1016/j.surfcoat.2017.02.001
22. Chen C, Xie X, Xie Y, Yan X, Huang C, Deng S, Ren Z, Liao H (2018) Metallization of polyether ether ketone (PEEK) by copper coating via cold spray. Surf Coat Technol 342:209–219. https://doi.org/10.1016/j.surfcoat.2018.02.087
23. Lupoi R, O'Neill W (2010) Deposition of metallic coatings on polymer surfaces using cold spray. Surf Coat Technol 205:2167–2173. https://doi.org/10.1016/j.surfcoat.2010.08.128
24. Vucko MJ, King PC, Poole AJ, Carl C, Jahedi MZ, de Nys R (2012) Cold spray metal embedment: an innovative antifouling technology. Biofouling 28:239–248. https://doi.org/10.1080/08927014.2012.670849
25. Sanpo N, Ang SM, Cheang P, Khor KA (2009) Antibacterial property of cold sprayed chitosan-Cu/Al coating. J Therm Spray Technol 18:600–608. https://doi.org/10.1007/s11666-009-9391-5
26. Sanpo N, Tan ML, Cheang P, Khor KA (2008) Antibacterial property of cold-sprayed HA-Ag/PEEK coating. J Therm Spray Technol 18:10–15. https://doi.org/10.1007/s11666-008-9283-0
27. Ogawa K, Ito K, Ichimura K, Ichikawa Y, Ohno S, Onda N (2008) Characterization of low-pressure cold-sprayed aluminum coatings. J Therm Spray Technol 17:728–735. https://doi.org/10.1007/s11666-008-9254-5
28. Che H, Chu X, Vo P, Yue S (2018) Metallization of various polymers by cold spray. J Therm Spray Technol 27:169–178. https://doi.org/10.1007/s11666-017-0663-1
29. Che H, Chu X, Vo P, Yue S (n.d.) Cold spray of mixed metal powders on carbon fibre reinforced polymers. Surf Coat Technol 329:232–243. https://doi.org/10.1016/j.surfcoat.2017.09.052
30. Raoelison RN, Aubignat E, Planche M-P, Costil S, Langlade C, Liao H (2016) Low pressure cold spraying under 6 bar pressure deposition: exploration of high deposition efficiency solutions using a mathematical modelling. Surf Coat Technol 302:47–55. https://doi.org/10.1016/j.surfcoat.2016.05.068
31. Tabbara H, Gu S, McCartney DG, Price TS, Shipway PH (2011) Study on process optimization of cold gas spraying. J Therm Spray Technol 20:608–620. https://doi.org/10.1007/s11666-010-9564-2
32. Faizan-Ur-Rab M, Zahiri SH, Masood SH, Phan TD, Jahedi M, Nagarajah R (2016) Application of a holistic 3D model to estimate state of cold spray titanium particles. Mater Des 89:1227–1241. https://doi.org/10.1016/j.matdes.2015.10.075
33. Raoelison RN, Aubignat E, Planche M-P, Costil S, Langlade C, Liao H (2016) Low pressure cold spraying under 6bar pressure deposition: exploration of high deposition efficiency solutions using a mathematical modelling. Surf Coat Technol 302:47–55. https://doi.org/10.1016/j.surfcoat.2016.05.068
34. Liberati AC, Che H, Vo P, Yue S (2019) Observation of an indirect deposition effect while cold spraying Sn-Al mixed powders onto carbon fiber reinforced polymers. J Therm Spray Technol 29:134–146. https://doi.org/10.1007/s11666-019-00967-w
35. Raoelison RN, Xie Y, Sapanathan T, Planche MP, Kromer R, Costil S, Langlade C (2018) Cold gas dynamic spray technology: a comprehensive review of processing conditions for various technological developments till to date. Addit Manuf 19:134–159. https://doi.org/10.1016/j.addma.2017.07.001
36. Winnicki M, Małachowska A, Dudzik G, Rutkowska-Gorczyca M, Marciniak M, Abramski K, Ambroziak A, Pawłowski L (2015) Numerical and experimental analysis of copper particles velocity in low-pressure cold spraying process. Surf Coat Technol 268:230–240. https://doi.org/10.1016/j.surfcoat.2014.11.059
37. Winnicki M, Małachowska A, Baszczuk A, Rutkowska-Gorczyca M, Kukla D, Lachowicz M, Ambroziak A (n.d.) Corrosion protection and electrical conductivity of copper coatings deposited by low-pressure cold spraying. Surf Coat Technol 318:90–98. https://doi.org/10.1016/j.surfcoat.2016.12.101
38. Lagerbom J, Koivuluoto H, Larjo J, Kylmälahti M, Vuoristo P (2007) Comparison of coatings prepared by two different cold spray processes, Beijing, China
39. Rokni MR, Feng P, Widener CA, Nutt SR (2019) Depositing Al-based metallic coatings onto polymer substrates by cold spray. J Therm Spray Technol 28:1699–1708. https://doi.org/10.1007/s11666-019-00911-y
40. Gülhan A, Braun S (2011) An experimental study on the efficiency of transpiration cooling in laminar and turbulent hypersonic flows. Exp Fluids 50:509–525. https://doi.org/10.1007/s00348-010-0945-6